NHR-8 regulated P-glycoproteins uncouple xenobiotic stress resistance from longevity in chemosensory *C. elegans* mutants

Gabriel A. Guerrero[1], Klara Schilling[1], Felix A.M.C. Mayr[1], Ryan Lu[4], Bérénice A. Benayoun[4] & Martin S. Denzel[1,2,3]*

[1]Max Planck Institute for Biology of Ageing
Joseph-Stelzmann-Str. 9b
D-50931 Cologne, Germany

[2]CECAD - Cluster of Excellence
University of Cologne
Joseph-Stelzmann-Str. 26
D-50931 Cologne, Germany

[3]Center for Molecular Medicine Cologne (CMMC)
University of Cologne
Robert-Koch-Str. 21
D-50931 Cologne, Germany

[4]Leonard Davis School of Gerontology
University of Southern California
Los Angeles, CA 90089, USA

*correspondence:
mdenzel@age.mpg.de

Abstract

Longevity is often associated with stress resistance, but whether they are causally linked is incompletely understood. Here we investigate chemosensory defective *Caenorhabditis elegans* mutants that are long-lived and stress resistant. We find that mutants in the intraflagellar transport protein gene *osm-3* are completely protected from tunicamycin-induced ER stress. While *osm-3* lifespan extension is fully dependent on the key longevity factor DAF-16/FOXO, tunicamycin resistance is not. *osm-3* mutants are protected from bacterial pathogens, which is fully *pmk-1* p38 MAP kinase dependent. Transcriptomic analysis revealed enhanced expression of P-glycoprotein xenobiotic detoxification genes in *osm-3* mutants and chemical inhibition of P-glycoproteins with verapamil suppressed tunicamycin resistance. Of note, the nuclear hormone receptor *nhr-8* is necessary and sufficient to regulate P-glycoproteins and tunicamycin resistance. We thus identify a cell-nonautonomous regulation of xenobiotic detoxification and show that separate pathways are engaged to mediate longevity, pathogen resistance, and xenobiotic detoxification in *osm-3* mutants.

42 **Introduction**

43 Chemosensation is a genetically tractable phenotype in various model
44 organisms. In *C. elegans*, many mutants with defective chemosensation have been
45 identified. Sensory phenotypes are complex in nature and many of the classical
46 chemosensory mutants were originally characterized by their behavioral phenotypes.
47 Odr mutants for example have an abnormal odorant response while Osm (osmotic
48 avoidance abnormal) mutants do not avoid high salt environments (Bargmann, 2006).
49 In mutants like *tax-4* and *odr-1*, mutations in components of neuronal G-protein
50 coupled receptor (GPCR) signaling cause atypical chemosensory behavior
51 (Bargmann, 2006). These mutants are not only characterized by a failure to adequately
52 respond to their environment, but show additional phenotypes linked to various life
53 traits including pathogen resistance, increased lifespan and drug detoxification (Gaglia
54 et al., 2012, Apfeld and Kenyon, 1999, Dent et al., 2000). Many chemosensory mutants
55 are long lived and this phenotype depends on the DAF-16/FOXO transcription factor
56 that is regulated by the insulin signaling pathway (Apfeld and Kenyon, 1999).

57 Beyond mutations in GPCRs, variants in genes involved in the development of
58 amphid sensory neurons can lead to chemosensory defects. One example are
59 mutations in intraflagellar transport (IFT) proteins that prevent full cilia development of
60 amphid sensory neurons (Inglis et al., 2007). Alterations in the IFT genes *osm-3* and
61 *daf-10* physically disrupt the development of neuronal dendrites that project toward the
62 tip of the nose where they are exposed to the outer environment (Inglis et al., 2007).
63 Thus, IFT mutants are usually characterized by defects in the chemical perception of
64 their environment. Further, developmental defects in lumen formation of the amphid
65 head channel in *daf-6* mutants prevent the direct contact of amphid sensory neurons
66 with the outside (Perens and Shaham, 2005).

67 In wild type (WT) worms, amphid and phasmid sensory neurons can be
68 visualized using the red lipophilic dye DiI, which fluorescently stains them bright red.
69 The dye is passively taken up by sensory neurons when they are fully developed and
70 in contact with the environment. Dye filling defective (Dyf) *C. elegans* are defined by
71 an inability to take up DiI into their sensory neurons (Inglis et al., 2007). The Dyf
72 phenotype arises in *daf-6* animals and also in many IFT mutants. Interestingly, Dyf
73 mutants have unique stress resistance phenotypes that act via different signaling
74 pathways. One such Dyf mutant, *daf-10(m79)*, has a unique resistance to pathogenic
75 bacteria that was proposed to be downstream of sensory input (Gaglia et al., 2012).
76 Further, pairs of amphid head neurons, such as ASH and ASJ that often become
77 disrupted in Dyf mutants help coordinate the innate immune response to bacterial
78 stress after infection (Meisel et al., 2014). Longevity is often associated with activation
79 of physiological stress pathways and has been shown to be regulated by the insulin
80 signaling pathway in Dyf *C. elegans* (Apfeld and Kenyon, 1999).

81 Conserved mechanisms of longevity and stress resistance have additionally
82 been linked to hyposmia in higher model organisms. In *Drosophila melanogaster*, loss
83 of the putative chemoreceptor *Or83b* has been shown to significantly increase lifespan
84 (Libert et al., 2007). Further, mice with ablated olfactory sensory neurons, have a
85 unique metabolic signature that protects them from high-fat diets (Riera et al., 2017).

86 While the olfactory machinery is seemingly more complex in higher organisms,
87 *C. elegans* have unique phenotypes associated with the loss or alteration of their
88 sensory neurons. First, unbiased screens for drug resistance have independently
89 identified the Dyf phenotype as a common feature in drug resistant *C. elegans* (Fujii et
90 al., 2004, Menez et al., 2016, Collins et al., 2008). Selection for resistance to the
91 anthelmintic drug ivermectin was shown to enrich for Dyf mutants in several forward
92 genetic screens (Menez et al., 2016, Page, 2018, Dent et al., 2000). Follow up work

93 identified P-glycoproteins, a class of ATP binding cassette (ABC) transporters, as the
94 drivers behind ivermectin resistance in Dyf mutants (Ardelli and Prichard, 2013).
95 Second, some chemosensory mutants, such as *daf-10*, show resistance to pathogenic
96 bacteria (Gaglia et al., 2012).

97 Here, we characterize a long-lived Dyf mutant, *osm-3*, that was previously
98 identified in a forward genetic screen for resistance to the potent ER stressor
99 tunicamycin (TM). From this screen, we reported the role of the hexosamine
100 biosynthetic pathway in TM resistance and longevity (Denzel et al., 2014). Our aim
101 was to uncover the mechanism by which Dyf mutants are resistant to TM.
102 Characterization of this phenotype demonstrates that TM resistance is independent
103 from the *osm-3* longevity and pathogen resistance phenotypes. Further, using
104 transcriptomics and functional analyses, we showed that P-glycoproteins mediate TM
105 resistance in Dyf animals. In addition, we found that the nuclear hormone receptor *nhr-*
106 *8* mediates *osm-3* drug resistance. Thus, our work highlights drug resistance as a
107 unique characteristic of Dyf mutants and functionally uncouples it from known stress
108 response pathways that have been implicated in stress resistance and longevity of
109 chemosensory mutants.

110 **Results**

111 **Dye filling defective *C. elegans* mutants are resistant to TM**

112 TM is commonly used to induce endoplasmic reticulum (ER) stress by inhibiting
113 the addition of N-glycans to nascent polypeptides (Parodi, 2000, Heifetz et al., 1979).
114 In *C. elegans*, where the ER machinery is conserved, treatment with TM is toxic and
115 induces the ER unfolded protein response. In fact, on plates containing TM at
116 concentrations above 4 μg/mL, newly hatched larvae die at early developmental
117 stages (Shen et al., 2001). Previously, we had carried out an ethyl methane-sulfonate
118 (EMS) mutagenesis screen to identify TM resistant *C. elegans* (Denzel et al., 2014).
119 The largest cohort of classifiable mutants presented dye filling defects (Dyf)
120 (Figure 1A). Dyf mutants are uniquely characterized by their inability to take up the
121 lipophilic red fluorescent dye DiI in their ciliated amphid neurons (Inglis et al., 2007).

122 Among the Dyf mutants from the TM resistance screen, we found new alleles
123 of genes previously linked to ciliary development. The mutant allele we selected for
124 our investigation, *osm-3(dh441) IV* (this allele will be referred to as *osm-3*), carries a
125 premature stop in the third exon, which prevents normal cilia development causing the
126 Dyf phenotype (Figure 1A, Supplementary Fig 1A;). *osm-3* is a member of the kinesin
127 family involved in axonal transport and development and mutants are known to show
128 a Dyf phenotype (Inglis et al., 2007). While WT worms fail to develop on TM at
129 concentrations above 4 μg/mL, *osm-3* mutants fully develop at concentrations at least
130 up to 10 μg/mL TM (Figure 1B). Loss of OSM-3, as well as other Dyf mutations,
131 promotes longevity in *C. elegans* (Apfeld and Kenyon, 1999). Demographic lifespan
132 analysis of *osm-3* indeed confirmed extended lifespan in our point mutant (Figure 1C
133 and Supplementary Table 1). *osm-3* mutants, and Dyf mutants in general, have never
134 been described as TM resistant especially at concentrations as high as 10 μg/mL.

135 To further explore whether the Dyf phenotype is linked to TM resistance we
136 tested other Dyf mutants that were previously described as long lived in the literature
137 (Apfeld and Kenyon, 1999). To our surprise, all Dyf mutants that we tested proved to
138 be significantly TM resistant (Figure 1D, 1F). On the other hand, the long-lived
139 chemosensory mutants *odr-1(n1936) X* and *odr-3(n2150) V* that display no Dyf
140 phenotype were only slightly TM resistant (Figure 1E, 1F). Our data thus suggest that,
141 among the larger class of chemosensory defective mutants, TM resistance is
142 specifically found in Dyf mutants.

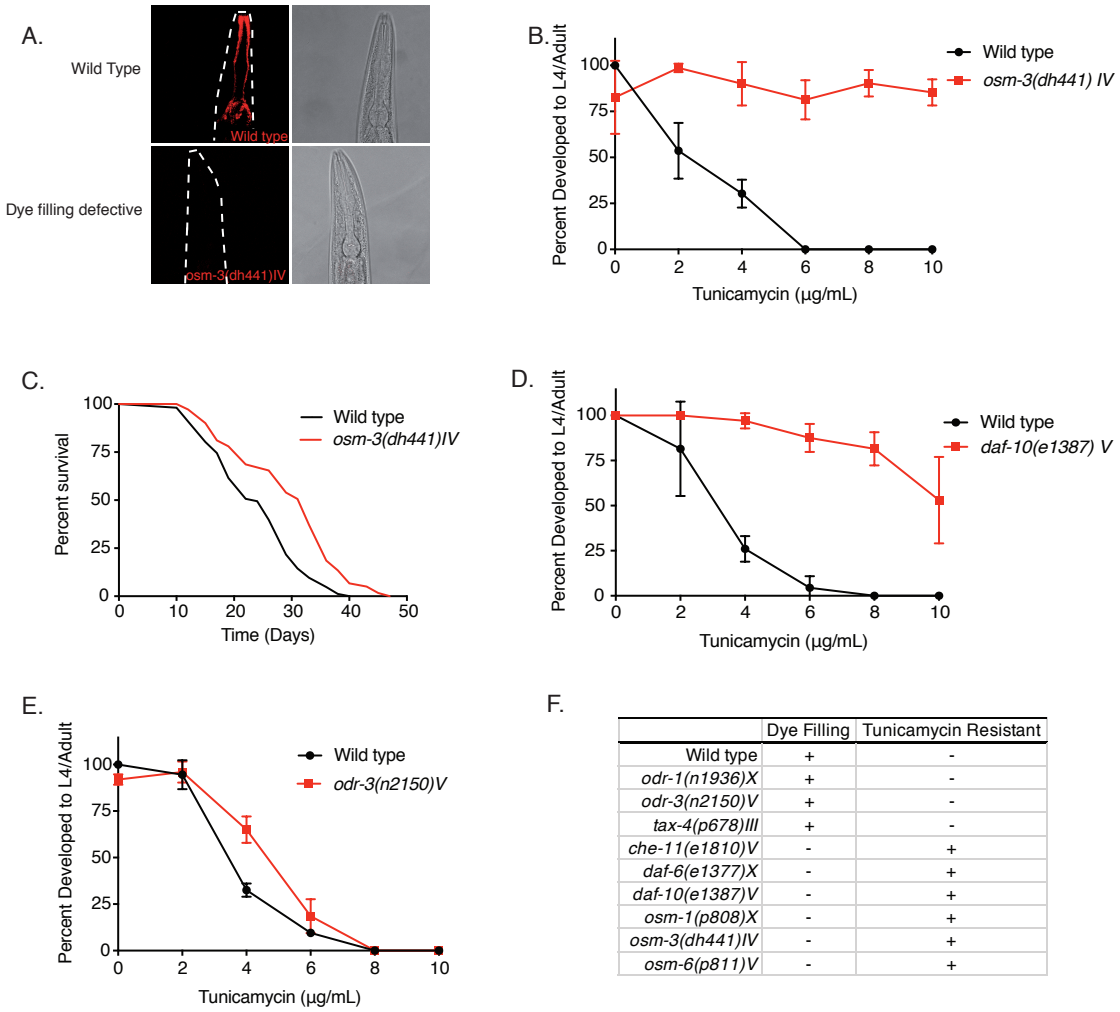

F.

	Dye Filling	Tunicamycin Resistant
Wild type	+	-
odr-1(n1936)X	+	-
odr-3(n2150)V	+	-
tax-4(p678)III	+	-
che-11(e1810)V	-	+
daf-6(e1377)X	-	+
daf-10(e1387)V	-	+
osm-1(p808)X	-	+
osm-3(dh441)IV	-	+
osm-6(p811)V	-	+

Figure 1. Dye filling defective *C. elegans* mutants are resistant to TM
A. Red fluorescence and differential interference contract confocal microscopy images of WT and *osm-3(dh441) IV C. elegans* after DiI treatment.
B. TM developmental assay with WT animals and *osm-3(dh441) IV* mutants.
C. Demographic lifespan analysis of WT and *osm-3(dh441) IV* animals. WT mean lifespan = 24 days, *osm-3(dh441) IV* mean lifespan = 29 days, $p < 0.0001$.
D. TM development assay with WT and *daf-10(e1387) V* mutants
E. TM development assay with WT and *odr-3(n2150) V* mutants
F. Table of dye filling phenotype and TM resistance. In the dye filling column, + is filled and - is Dyf. In the TM resistant column, + is resistant and - is not resistant to 10 µg/mL TM.

143

144 **ER stress response is blunted in *osm-3* mutants**

145 TM treatment activates the ER unfolded protein response (ER UPR); we thus
146 characterized the overall transcriptional response of *osm-3* mutants upon TM
147 treatment. We performed transcriptomic analysis on *osm-3* and WT worms after
148 6 hours of TM treatment. Notably, the gene ontology (GO) terms related to ER stress
149 and ER protein folding showed significant upregulation in WT animals but not in *osm-*
150 *3* mutants (Figure 2A). qPCR analysis of UPR target genes further confirmed that there
151 was no ER UPR induction in the TM-treated *osm-3* mutants compared to the WT
152 (Supplementary Figure 2). A hallmark of ER UPR induction in *C. elegans* is the
153 upregulation of the molecular chaperone HSP-4/BiP (Shen et al., 2001). Upon TM
154 treatment of *osm-3* mutants carrying a *hsp-4*::GFP reporter, there was no significant
155 increase in the GFP signal compared to the untreated control, while in the WT the GFP
156 levels were significantly increased (Figure 2A, 2B). This observation corroborates the
157 results from the transcriptome analysis.

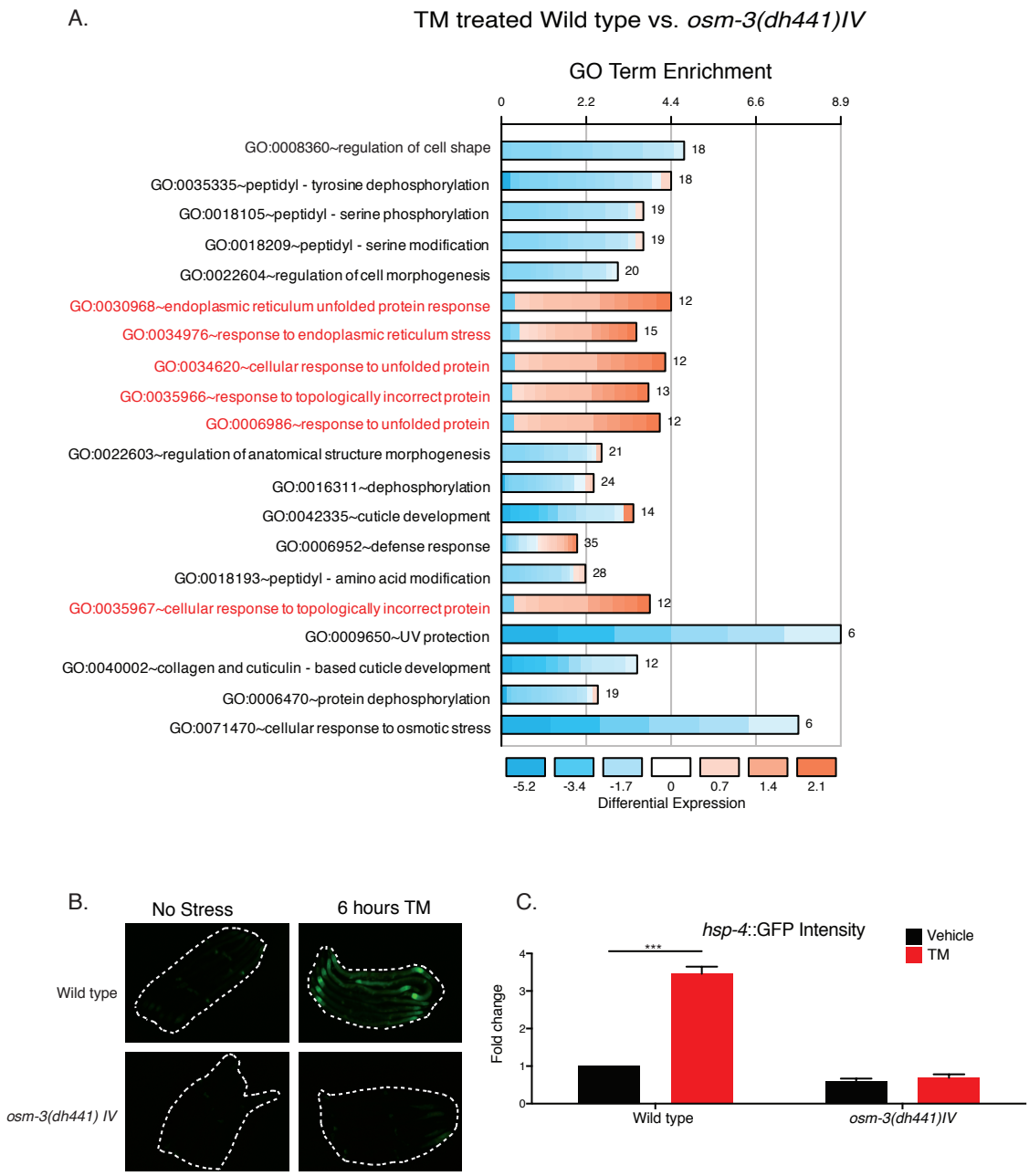

Figure 2. ER stress response is blunted in *osm-3* mutants

A. DAVID gene ontology (GO) terms that are enriched in TM-treated WT compared to TM-treated *osm-3(dh441) IV* worms. Red GO terms are upregulated and blue downregulated.

B. Green fluorescent images of WT and *osm-3(dh441) IV* animals in the *hsp-4*::GFP background after 6 hours of 10 μg/mL TM treatment. Worms are outlined in the images.

C. Biosorter analysis of *osm-3(dh441) IV* vs. WT animals in the *hsp-4*::GFP background after 6 hours of control or TM treatment. Data are mean + SEM, n = 4, *** $p<0.0001$ by two-way ANOVA.

158

159 **TM resistance in *osm-3* mutants is not mediated through *daf-16* or PMK-1/p38**
160 **MAPK pathway**

161 The lifespan extension observed in chemosensory defective *C. elegans* as well
162 as in *Drosophila* has been shown to be at least partially insulin signaling dependent
163 (Apfeld and Kenyon, 1999, Libert et al., 2007). Therefore, we performed a
164 demographic lifespan analysis to determine the role of the insulin signaling pathway in
165 the lifespan extension of *osm-3* mutants. Indeed, the *osm-3* lifespan extension was
166 fully *daf-16* dependent, as the lifespan of the *osm-3; daf-16* double mutants was
167 identical to the *daf-16* lifespan (Figure 3A and Supplementary Table 1). To our
168 surprise, the *osm-3; daf-16* double mutant was resistant to TM while *daf-16* single
169 mutants do not develop at 10 μg/mL TM (Figure 3B). Further, knock-down of *daf-16* by
170 RNA interference did not rescue the *hsp-4*::GFP response after TM treatment
171 (Figure 3C). Given previous links between the insulin signaling pathway and the ER
172 stress signaling (Henis-Korenblit et al., 2010, Kyriakakis et al., 2017, Matai et al., 2019,
173 Labbadia and Morimoto, 2014), we were surprised to find that *daf-2* mutants failed to
174 develop on 10 μg/mL TM while *osm-3* mutants fully developed (Figure 3D). Together,
175 this evidence suggests that the *osm-3* lifespan extension and TM drug resistance are
176 uncoupled and instead appear to act via independent or parallel pathways.

177 In *C. elegans, Pseudomonas aeruginosa* PA14 is a pathogen that is often used
178 to study innate immunity. Of note, ER UPR targets have been implicated in the innate
179 immune response of *C. elegans* during PA14 infection (Richardson et al., 2010,
180 Haskins et al., 2008). As the ER thus plays a role in innate immunity and as TM disrupts
181 ER function, we speculated that *osm-3* mutants would be more robust on PA14 than
182 WT. Indeed, *osm-3* mutants were more resistant to PA14 than WT, however this
183 increased pathogen resistance was fully explained by the PMK-1 p38 mitogen-
184 activated protein kinase (MAPK) pathway (Figure 3E). With this in mind, we tested

185 whether *pmk-1* mutation could suppress the *osm-3* TM resistance. The *osm-3; pmk-1*
186 double mutant was fully resistant to TM, while the *pmk-1* single was fully sensitive
187 (Figure 3F). Taken together, insulin signaling and the MAPK pathway, two major stress
188 response pathways in *C. elegans* that have links to ER protein quality control,
189 seemingly have no impact on *osm-3*'s TM resistance.

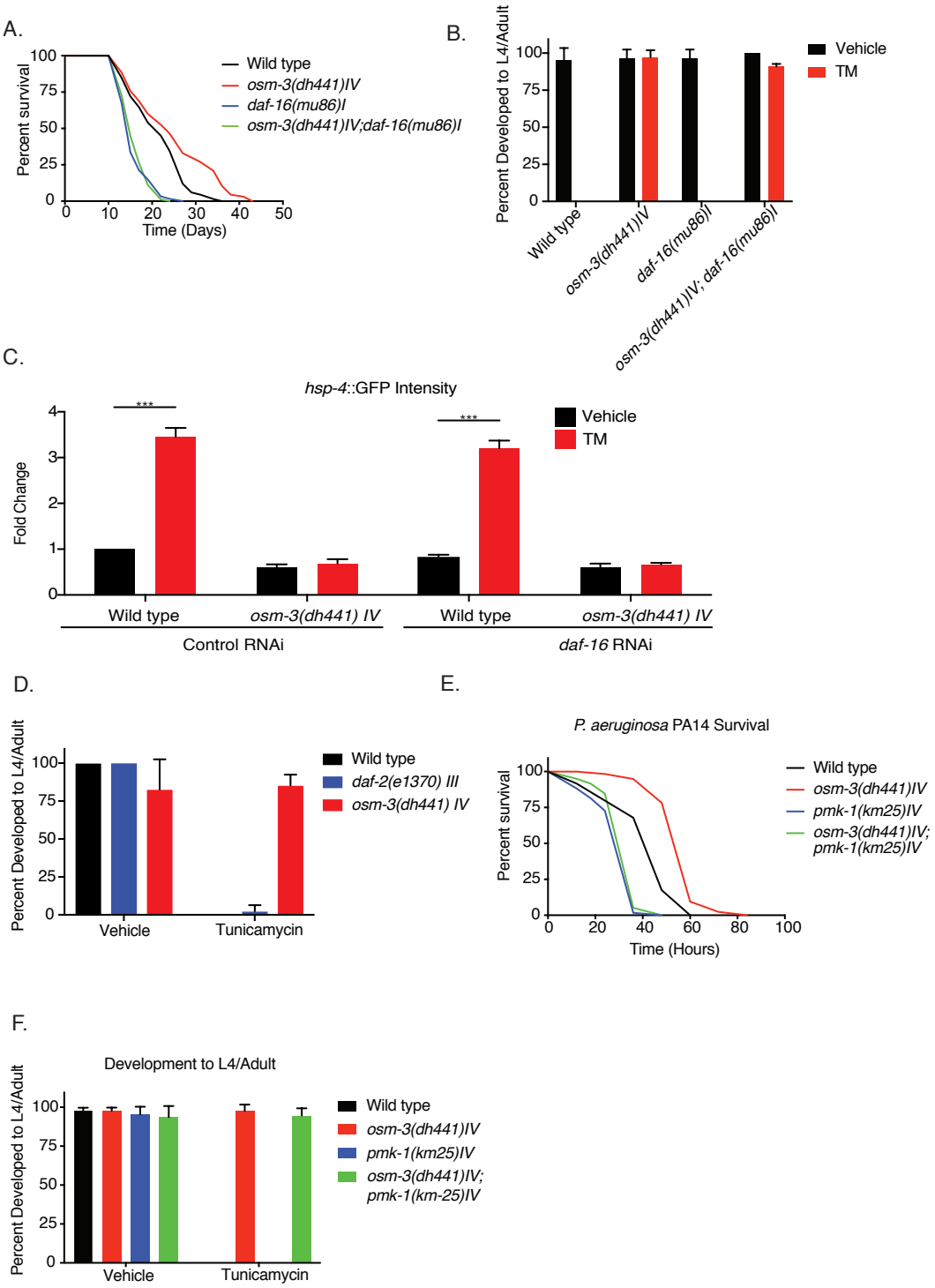

Figure 3. TM resistance in *osm-3* mutants is not *daf-16* or *pmk-1* dependent

A. Demographic lifespan analysis of WT, *osm-3(dhh441) IV*, *daf-16(mu86) I* and *osm-3(dh441) IV; daf-16(mu86) I* animals. WT mean lifespan = 22 days, *osm-3(dh441) IV* mean lifespan = 25 days $p < 0.005$ compared to WT, *daf-16(mu86) I* mean lifespan = 16 days $p < 0.0001$ compared to WT, *osm-3(dh441) IV*; *daf-16(mu86) I* mean lifespan = 16 days $p < 0.0001$ compared to WT.

B. TM developmental assay with WT, *osm-3(dh441) IV*, *daf-16(mu86) I*, and *osm-3(dh441) IV; daf-16(mu86) I* animals.

C. Biosorter analysis of *osm-3(dh441) IV* vs. WT in the *hsp-4*::GFP background raised on control or *daf-16* RNAi plates after 6 hours of control or TM treatment. Data are mean + SEM, n = 4, *** $p<0.001$ by two-way ANOVA.

D. TM developmental assay with WT, *osm-3(dh441) IV* and *daf-2(e1370) III* animals.

E. *Pseudomonas aeruginosa* PA14 survival assay with WT, *osm-3(dh441) IV*, *pmk-1(km25) IV*, and *osm-3(dh441) IV; pmk-1(km25) IV* animals. WT mean survival = 44 hours, *osm-3(dh441) IV* mean

survival = 58 hours p <0.001 compared to WT, *pmk-1(km25) IV* mean survival = 31 hours p <0.001 compared to WT, *osm-3(dh441) IV; pmk-1(km25) IV* mean survival = 34 hours p <0.001 compared to WT and p = 0.06 compared to *pmk-1(km25) IV*.

F. TM developmental assay with WT, *osm-3(dh441) IV*, *pmk-1(km25) IV*, and *osm-3(dh441) IV; pmk-1(km25) IV* animals.

190

191 **P-glycoproteins are significantly enriched in *osm-3* mutants**

192 The unique nature of Dyf drug resistance led us to investigate differences in
193 overall gene expression under basal conditions. Our transcriptomic analysis revealed
194 differential expression of P-glycoproteins (PGPs) in unstressed *osm-3* mutants
195 compared to WT. Specifically, we found that the PGPs *pgp-2*, *pgp-4* and *pgp-14* were
196 significantly upregulated in *osm-3* (Figure 4A). PGPs are a conserved family of ATP
197 binding cassette (ABC) transporters found on the cell membrane (Sangster, 1994).
198 *C. elegans* have 15 PGP genes. A comparison between control and TM treated WT
199 and *osm-3* mutants showed no further enrichment of these PGPs upon TM treatment
200 (Figure 4B). These findings led us to ask whether PGP upregulation is the driver of TM
201 drug resistance in *C. elegans*.

202

203 **P glycoprotein inhibition suppresses *osm-3* TM resistance**

204 We tested whether elevated PGP expression might be responsible for the
205 xenobiotic stress resistance in *osm-3* mutants. The PGP inhibitor verapamil (VPL) has
206 been used to specifically inhibit PGP activity, re-sensitizing worms to the antihelmintic
207 compound ivermectin (Menez et al., 2016). Indeed, 1 nM VPL significantly suppressed
208 development of *osm-3 C. elegans* in the presence of TM, while having no effect on
209 controls without TM (Figure 4C).

210 Dyf *C. elegans* mutants have been independently identified in drug resistance
211 screens (Fujii et al., 2004, Menez et al., 2016, Dent et al., 2000). Consistent with these
212 findings, we observed that *osm-3* mutants were resistant to 200 nM methyviologen
213 dichloride (paraquat), as they fully develop at a concentration that is toxic to WT
214 *C. elegans* (Figure 4D). Similarly, *osm-3* mutants fully developed to adults in the
215 presence of 6 μg/mL ivermectin that is lethal to WT (Figure 4E). In contrast, *osm-3*
216 mutants showed no difference to WT animals in heat stress assays or in the presence

217 of hydrogen peroxide (H_2O_2) suggesting that *osm-3* mutants are not resistant to non-
218 xenobiotic stressors (Supplementary Figure 4A, 4B). Together, these observations
219 suggest that *osm-3* mutants, and potentially Dyf mutants as a group, are significantly
220 resistant to xenobiotic stress.

221 Having explained the TM resistance of *osm-3* mutants through PGP dependent
222 xenobiotic detoxification, we wondered about its role in the longevity of *osm-3* mutants.
223 Notably, VPL did not shorten *osm-3* lifespan. Moreover, VPL did not affect WT lifespan
224 (Figure 4F and Supplementary Table 1) and had no visible effect on WT development
225 (Supplementary Figure 4C). Together, these data support the conclusion that the
226 xenobiotic stress resistance and longevity phenotypes of *osm-3* mutants are mediated
227 by fully independent pathways.

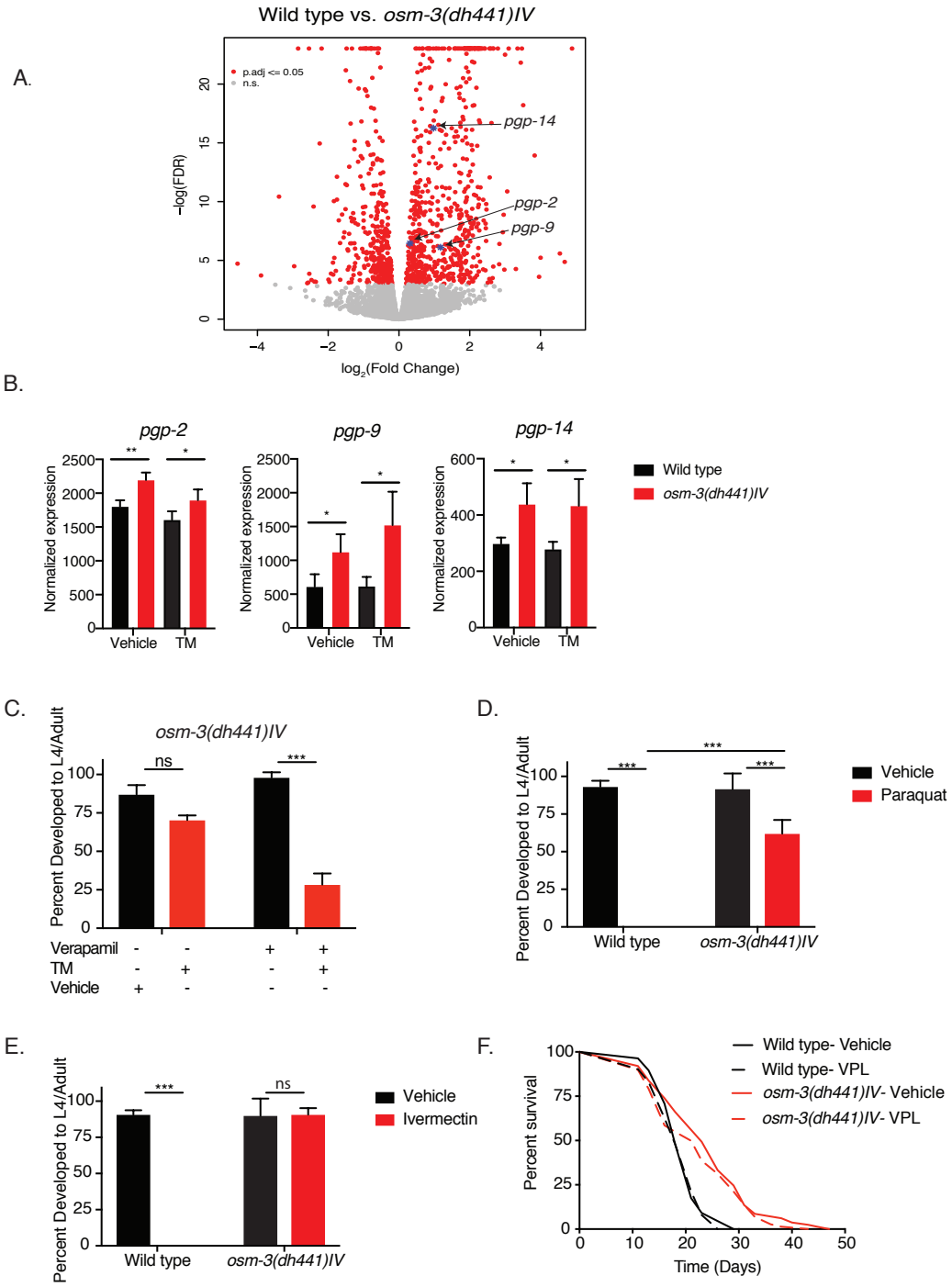

Figure 4. P-glycoproteins are significantly enriched in *osm-3* mutants

A. Volcano plot showing the global transcriptional changes in *osm-3(dh441) IV* compared to WT animals; *pgp-2*, *pgp-9* and *pgp-14* are labeled.

B. *pgp-2*, *pgp-9* and *pgp-14* expression levels in control and TM treated animals from transcriptomic data. Data are mean + SD, n = 4, * p<0.05, ** p<0.005 by t-test.

C. Verapamil (VPL) supplementation assay for development on TM using 10 μg/mL TM supplemented with vehicle or 1 nM VPL. Data are mean + SD, n = 3, *** p < 0.001 by two-way ANOVA.

D. Paraquat developmental assay of WT and *osm-3(dh441) IV* mutants using 0.2 mM paraquat and a vehicle control. Data are mean + SD, n = 3, *** p < 0.001 by two-way ANOVA.

E. Ivermectin developmental assay of WT and *osm-3(dh441) IV* mutants using 6 ng/mL ivermectin and a vehicle control. Data are mean + SD, n = 3, *** p < 0.001 by two-way ANOVA.

F. Demographic lifespan analysis on vehicle and VPL treated WT and *osm-3(dh441) IV* worms. Vehicle treated: WT mean lifespan = 19 days; *osm-3(dh441) IV* mean lifespan = 24 days p < 0.0001

compared to WT vehicle. VPL treated: WT mean lifespan = 19 days; *osm-3(dh441) IV* mean lifespan = 22 days, $p < 0.005$ compared to WT Vehicle.

228

229 **NHR-8 signaling regulates xenobiotic detoxification response through PGPs**

230 The nuclear hormone receptor NHR-8 has been linked to xenobiotic
231 detoxification and PGP regulation in *C. elegans* (Menez et al., 2019, Lindblom et al.,
232 2001). Indeed, using quantitative PCR we found that the upregulation of PGP
233 expression in *osm-3* mutants was suppressed in the *osm-3; nhr-8* double mutant
234 (Figure 5A). This led us to ask whether *osm-3* TM resistance was dependent on NHR-
235 8 signaling. Indeed, the *osm-3; nhr-8(hd117) IV* double mutant was not resistant to TM
236 while the *osm-3* mutant fully developed (Figure 5B), suggesting that NHR-8 is
237 necessary for *osm-3* TM resistance. We next asked if NHR-8 is sufficient for TM
238 resistance using a transgenic overexpressor line (Magner et al., 2013). Indeed, we
239 found that overexpression of *nhr-8* in WT worms results in significant TM resistance
240 (Figure 5C).

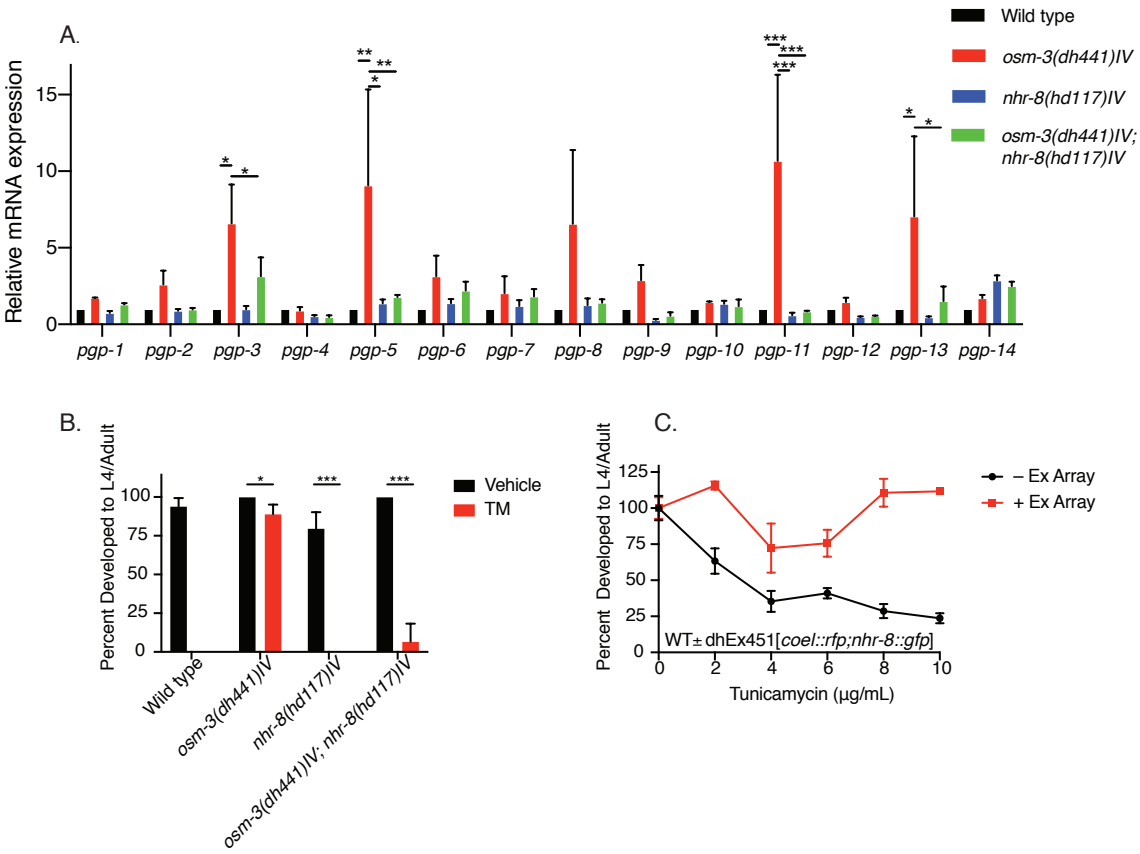

Figure 5. *nhr-8* signaling regulates xenobiotic detoxification response through PGPs
A. Quantitative PCR measuring relative PGP mRNA expression in WT, *osm-3(dh441) IV*, *nhr-8(hd117) IV* and *osm-3(dh441) IV; nhr-8(hd117) IV* animals. Data are mean + SEM, n = 3, * $p < 0.05$, ** $p < 0.001$, *** $p < 0.0001$ by two-way ANOVA.
B. TM developmental assay on 10 µg/mL TM and control with WT, *osm-3(dh441) IV*, *nhr-8(hd117) IV* and *osm-3(dh441) IV; nhr-8(hd117) IV* animals. Data are mean + SD, n = 3, * $p < 0.05$, *** $p < 0.0001$ by t-test.
C. TM developmental assay with transgenic animals containing an *nhr-8* overexpressing extrachromosomal array dhEx451[*coel::rfp;nhr-8::gfp*]. "-Ex Array" do not visibly contain the extrachromosomal array as judged by the co-injection marker and "+Ex Array" contain the extrachromosomal array. Data are mean + SEM, n = 3, * $p<0.05$ and *** $p < 0.005$ by two-way ANOVA.

241

242 **Discussion**

243 In this study, we found that Dyf mutants are resistant to the ER toxin TM. Instead
244 of an activated stress signaling status that might explain the TM resistance, *osm-3* Dyf
245 mutants show no ER UPR induction upon TM treatment. Consistent with previous
246 findings (Apfeld and Kenyon, 1999) the lifespan extension of *osm-3* was *daf-16*
247 dependent. Despite the established link between the insulin signaling pathway and
248 stress resistance, the TM resistance in *osm-3* mutants was not insulin signaling
249 dependent. Further, while *osm-3* mutants were pathogen resistant, this resistance was
250 fully dependent on the PMK-1/p38 MAPK pathway. We were surprised that neither of
251 the two pathways weakened the TM resistance phenotype. Dyf *C. elegans* drug
252 resistance is not specific to TM, as we also observed resistance to paraquat and
253 ivermectin. While paraquat and ivermectin resistance have been previously reported
254 in Dyf mutants (Dent et al., 2000, Fujii et al., 2004, Menez et al., 2016), no studies
255 have demonstrated similar resistance mechanisms in Dyf *C. elegans* mutants to TM.
256 Our findings show that this resistance is due to increased PGP expression in Dyf
257 worms. Importantly, we demonstrate regulation of PGPs by the nuclear hormone
258 receptor NHR-8. Broad inhibition of PGPs using verapamil or loss of *nhr-8* significantly
259 resensitized *osm-3* mutants to TM. Consistently, NHR-8 overexpression resulted in TM
260 resistance in WT animals. These data show that *nhr-8* is necessary and sufficient for
261 TM resistance.

262 Given that improved protein homeostasis is one of the cellular hallmarks of
263 longevity (Lopez-Otin et al., 2013), we presumed that selection for TM resistance
264 would serve as a proxy phenotype for longevity given that TM specifically targets ER
265 protein folding. More specifically, we expected that high fidelity ER protein quality
266 control would be the driver of longevity in these mutants. Previous findings describing
267 increased hexosamine biosynthetic pathway flux (Denzel et al., 2014) or constitutive

268 XBP-1 activation (Taylor and Dillin, 2013) have linked protein homeostasis to longevity
269 and stress resistance; therefore the connection between TM resistance and longevity
270 seemed apparent. Given that Dyf mutants are resistant to pathogenic bacteria through
271 enhanced ER homeostasis, we also speculated that TM resistance might serve as a
272 proxy phenotype for pathogen resistance. On the contrary, we found that increased
273 PGP expression is sufficient to drive detoxification in TM resistance but not longevity
274 in *osm-3* mutants. *pmk-1* and *daf-16* were behind pathogen resistance and longevity,
275 respectively.

276 Adding another dimension to the cell-nonautonomous regulation of innate
277 immunity (Aballay, 2013), we propose that the nervous system regulates systemic
278 xenobiotic detoxification *C. elegans*. Our data suggest that mutants with defective
279 amphid neurons have increased PGP expression. Several PGPs have been shown to
280 be expressed in non-neuronal tissue (Lincke et al., 1993, Sheps et al., 2004).
281 Moreover, we found that PGP expression is regulated by *nhr-8*, which has also been
282 shown to be expressed in the intestine of *C. elegans* (Magner et al., 2013). Combining
283 this previous information with our finding that Dyf mutants are resistant to several
284 uniquely toxic drugs, we conclude that neuronal signaling controls drug resistance
285 through nuclear hormone signaling. To this end one might further investigate the link
286 between neuronal states and the cholesterol-derived signal that drives these drug
287 resistance phenotypes.

288 PGPs are likely regulated in *C. elegans* to help them combat toxins found in
289 their natural habitat. Toxic metabolites are undoubtedly common in the soil where
290 *C. elegans* are found. The drugs used in our study, ivermectin (a derivative of
291 avermectin) (Burg et al., 1979) and TM, were first discovered as antibiotics that are
292 produced by soil bacteria (Takatsuki et al., 1971). Because *C. elegans* have no
293 adaptive immune response, having PGPs as part of their innate immune system allows

294 them to clear toxic molecules they may encounter in the wild. While Dyf mutants do
295 not occur in the wild, our data nonetheless demonstrate a link environmental sensing
296 and drug resistance.

297 In humans, PGPs have been implicated in drug resistant malignancies (Lehne,
298 2000). Using *C. elegans* as a tool to study the cross talk between tissues, one might
299 be able to better understand how extracellular signaling drives ABC transporter
300 expression in chemotherapy resistant cancer. Further studies in cell culture might also
301 further characterize TM, as well as other toxic metabolites, as substrates for *C. elegans*
302 PGPs.

303 **Materials and Methods**

304

305 **Worm maintenance**

306 *C. elegans* nematodes were cultured using standard husbandry methods at
307 20°C on nematode growth media (NGM) agar plates seeded with *E. coli* strain OP50
308 unless otherwise stated (Brenner, 1974).

309

310 **Dye filling assay in *C. elegans***

311 The dye filling assay was performed on a synchronized population of day 1
312 adults. 40-60 adult worms were placed in M9 containing 10 μg/mL DiI. They were left
313 at room temperature for two hours in the staining medium, then transferred to NGM
314 plates seeded with *E. coli* OP50. The worms were then allowed to crawl on the food
315 for one hour to allow for the dye to be cleared from the gut. The worms were scored
316 for dye filling using a Leica SPX-8 confocal microscope or a Leica fluorescent stereo-
317 microscope. Images were taken using the confocal microscope.

318

319 **Drug resistance assays**

320 NGM plates containing either TM, paraquat or ivermectin were used in
321 developmental assays to test for resistance. To this end, we performed a 4h egg lay
322 on NGM plates at room temperature then transferred the eggs to control and drug
323 containing plates and recorded the number of eggs per plate. After incubation for four
324 days at 20°C, plates were scored by counting the total number of L4 larvae or adults
325 on each plate. Paraquat plates were prepared by adding 1M methyl viologen dichloride
326 (paraquat) directly onto seeded NGM plates for a final concentration of 200 μM and
327 allowed to dry immediately before use. Ivermectin plates were prepared by adding
328 ivermectin directly to the NGM medium at a final concentration of 6 μg/mL before

329 pouring the plates. Modified NGM plates containing no cholesterol were made by using
330 standard NGM without the addition of cholesterol. These modified NGM plates were
331 then supplemented with drugs as described above. All of the drug development assays
332 were performed using *E. coli* OP50 bacteria.
333
334 **ER stress quantification by *hsp-4*::GFP**
335 Synchronized day 1 adults were transferred to control and TM containing NGM
336 plates seeded with OP50. After 6 hours of stress induction *hsp-4*::GFP levels were
337 measured by large particle flow cytometry in both the WT and *osm-3(dh441)IV*
338 background using the Union Biometrica Biosorter. For *daf-16* knockdown by RNAi,
339 animals were raised on control and *daf-16* RNAi. Synchronized day 1 adults were
340 transferred to control or TM containing plates seeded with control or *daf-16* RNAi. After
341 6 hours of stress, GFP levels were measured using the Biosorter. GFP values were
342 normalized to time of flight.
343
344 **Quantitative PCR**
345 For ER stress induction day 1 adults were washed from their plates and
346 transferred to either control or TM containing plates, where they were incubated for 6h.
347 The animals were then washed off using M9 and snap frozen in trizol. Unstressed
348 synchronized animals were collected at day 1 of adult hood for RNA extraction. RNA
349 was prepared using Zymo Research Direct-zol RNA Microprep kit. SYBR green was
350 used to perform quantitative PCR (RT-qPCR). See Supplementary Materials for list of
351 qPCR primers used in this study.

352 **Lifespan analysis**

353 Adult lifespan analysis was performed at 20°C on mutant and WT *C. elegans*.
354 The animals were synchronized in a four-hour egg lay. Animals were scored as dead
355 or alive every second day until the end of the experiment. Animals were transferred
356 every day for the first seven days. Statistical analysis on the Kaplan-Meier survival
357 curves was performed using Microsoft Excel. See Supplementary Materials for lifespan
358 statistics.

359

360 **Hydrogen peroxide survival assay**

361 1M hydrogen peroxide (H_2O_2) was added to unseeded NGM plates to a final
362 concentration of 1 μM and allowed to dry for several minutes. Synchronized day one
363 adults were then transferred onto the plates and incubated at 25°C. The animals were
364 then scored every 2 hours for survival.

365

366 **Pathogenic bacteria survival assay**

367 The *Pseudomonas aeruginosa* strain PA14 was grown in LB media and seeded
368 onto high peptone NGM plates and incubated for 12 hours at 37°C immediately before
369 the start of the experiment. Day one animals were first transferred to unseeded NGM
370 plates to crawl around the plate and remove any excess *E. coli* OP50 off of their bodies.
371 They were then transferred to the PA14 containing plates and incubated at 25°C. The
372 animals were scored every 12 hours until all animals were dead.

373

374 **Heat stress survival assay**

375 Day 1 synchronized *C. elegans* were transferred to fresh NGM plates seeded
376 with *E. coli* OP50. These plates were transferred to a 35°C incubator, where they were

377 evenly distributed throughout the incubator to ensure even heat exposure. The plates
378 were scored for live worms every 2 hours until all of the worms were dead.
379
380 **Sample collection and RNA purification for sequencing**
381 For RNA sequencing we used day one adults that were hatched within one hour.
382 To achieve this synchronization, we washed all adults and larvae of plates with M9 and
383 allowed the eggs on hatch for one hour. The freshly hatched L1 larvae were then
384 washed off and transferred to fresh plates seeded with OP50 and incubated at 20°C
385 until they developed to adults. At day one of adulthood, animals were washed from
386 their plates and transferred to either control or TM containing plates, where they were
387 incubated for 6 hours. The animals were then washed off using M9 and snap frozen in
388 trizol. All biological replicates were collected and prepared using a snaking collection
389 method to reduce batch effects. Total RNA was purified using Zymo Research Direct-
390 zol RNA Microprep kit.
391
392 **RNA-seq library preparation**
393 RNA quality was assessed using Agilent's Bioanalyzer platform, and samples
394 with RIN > 9 were used for library construction. 2.5 µg of total RNA was subjected to
395 ribosomal RNA (rRNA) depletion using the Illumina's Ribo-zero Gold kit (Illumina),
396 according to the manufacturer's protocol. Strand specific RNA-seq libraries were then
397 constructed using the SMARTer Stranded RNA-Seq HT Kit (Clontech #634839),
398 according to the manufacturer's protocol. Based on rRNA-depleted input amount, 15
399 cycles of amplification were performed to generate RNA-seq libraries. Paired-end
400 150 bp reads were sent for sequencing on the Illumina HiSeq-Xten platform at the
401 Novogene Corporation (USA). The resulting data was then analyzed with a
402 standardized RNA-seq data analysis pipeline (described below).

403 **RNA-seq analysis pipeline**

404 cDNA sequences of worm genes were obtained through ENSEMBL Biomart for
405 the WBCel235 build of the *C. elegans* genome (Ensemble release v94; accessed
406 2018-12-03). Trimmed reads were mapped to this reference using kallisto 0.43.0-1 and
407 the –fr-stranded option (Bray et al., 2016). All subsequent analyses were performed in
408 the R statistical software (https://cran.r-project.org/). Read counts were imported into
409 R, and summarized at the gene level. Differential gene expression was estimated using
410 the 'DESeq2' R package (DESeq2 1.16.1) [PMID: 25516281]. David analysis (version
411 6.8) was performed to identify significantly enriched gene ontology terms.

412

413 **Developmental verapamil (VPL) resistance assay and lifespan analysis**

414 Plates containing 10 μg/mL TM were supplemented with 1 nM VPL by adding
415 VPL solved in DMSO onto the plates. Plates were allowed to dry for 6h before eggs
416 were transferred to them to determine developmental resistance to TM. Plates were
417 then scored after 4 days to determine the relative number of L4 larvae or adults.
418 Lifespan assays were performed as above, however the animals were transferred to
419 fresh VPL containing plates every second day for the whole lifespan assay.

Acknowledgements

We thank all M.S.D. laboratory members for lively and helpful discussions. We thank Adam Antebi for valuable comments and for *C. elegans* strains. We thank Seung-Jae Lee for valuable comments on the manuscript. We thank the Caenorhabditis Genetics Center (CGC) for strains. We thank the members of the bioinformatics core facility and the FACS and imaging core facility at MPI AGE. B.A.B is supported by a seed grant from the NAVIGAGE foundation, and a generous gift from the Hanson-Thorell Family. M.S.D. was supported by ERC-StG 640254, by the Deutsche Forschungsgemeinschaft (DFG, German Research Foundation) - Projektnummer 73111208 - SFB 829, and by the Max Planck Society.

Competing interests

The authors declare no competing interests.

433 **References**

434 ABALLAY, A. 2013. Role of the nervous system in the control of proteostasis during innate
435 immune activation: insights from C. elegans. *PLoS Pathog,* 9**,** e1003433.
436 APFELD, J. & KENYON, C. 1999. Regulation of lifespan by sensory perception in
437 Caenorhabditis elegans. *Nature,* 402**,** 804-9.
438 ARDELLI, B. F. & PRICHARD, R. K. 2013. Inhibition of P-glycoprotein enhances sensitivity of
439 Caenorhabditis elegans to ivermectin. *Vet Parasitol,* 191**,** 264-75.
440 BARGMANN, C. I. 2006. Chemosensation in C. elegans. *WormBook***,** 1-29.
441 BRAY, N. L., PIMENTEL, H., MELSTED, P. & PACHTER, L. 2016. Near-optimal probabilistic RNA-
442 seq quantification. *Nat Biotechnol,* 34**,** 525-7.
443 BRENNER, S. 1974. The genetics of Caenorhabditis elegans. *Genetics,* 77**,** 71-94.
444 BURG, R. W., MILLER, B. M., BAKER, E. E., BIRNBAUM, J., CURRIE, S. A., HARTMAN, R., KONG,
445 Y. L., MONAGHAN, R. L., OLSON, G., PUTTER, I., TUNAC, J. B., WALLICK, H., STAPLEY,
446 E. O., OIWA, R. & OMURA, S. 1979. Avermectins, new family of potent anthelmintic
447 agents: producing organism and fermentation. *Antimicrob Agents Chemother,* 15**,**
448 361-7.
449 COLLINS, J. J., EVASON, K., PICKETT, C. L., SCHNEIDER, D. L. & KORNFELD, K. 2008. The
450 anticonvulsant ethosuximide disrupts sensory function to extend C. elegans lifespan.
451 *PLoS Genet,* 4**,** e1000230.
452 DENT, J. A., SMITH, M. M., VASSILATIS, D. K. & AVERY, L. 2000. The genetics of ivermectin
453 resistance in Caenorhabditis elegans. *Proc Natl Acad Sci U S A,* 97**,** 2674-9.
454 DENZEL, M. S., STORM, N. J., GUTSCHMIDT, A., BADDI, R., HINZE, Y., JAROSCH, E., SOMMER,
455 T., HOPPE, T. & ANTEBI, A. 2014. Hexosamine pathway metabolites enhance protein
456 quality control and prolong life. *Cell,* 156**,** 1167-1178.
457 FUJII, M., MATSUMOTO, Y., TANAKA, N., MIKI, K., SUZUKI, T., ISHII, N. & AYUSAWA, D. 2004.
458 Mutations in chemosensory cilia cause resistance to paraquat in nematode
459 Caenorhabditis elegans. *J Biol Chem,* 279**,** 20277-82.
460 GAGLIA, M. M., JEONG, D. E., RYU, E. A., LEE, D., KENYON, C. & LEE, S. J. 2012. Genes that act
461 downstream of sensory neurons to influence longevity, dauer formation, and
462 pathogen responses in Caenorhabditis elegans. *PLoS Genet,* 8**,** e1003133.
463 HASKINS, K. A., RUSSELL, J. F., GADDIS, N., DRESSMAN, H. K. & ABALLAY, A. 2008. Unfolded
464 protein response genes regulated by CED-1 are required for Caenorhabditis elegans
465 innate immunity. *Dev Cell,* 15**,** 87-97.
466 HEIFETZ, A., KEENAN, R. W. & ELBEIN, A. D. 1979. Mechanism of action of tunicamycin on
467 the UDP-GlcNAc:dolichyl-phosphate Glc-NAc-1-phosphate transferase. *Biochemistry,*
468 18**,** 2186-92.
469 HENIS-KORENBLIT, S., ZHANG, P., HANSEN, M., MCCORMICK, M., LEE, S. J., CARY, M. &
470 KENYON, C. 2010. Insulin/IGF-1 signaling mutants reprogram ER stress response
471 regulators to promote longevity. *Proc Natl Acad Sci U S A,* 107**,** 9730-5.
472 INGLIS, P. N., OU, G., LEROUX, M. R. & SCHOLEY, J. M. 2007. The sensory cilia of
473 Caenorhabditis elegans. *WormBook***,** 1-22.
474 KYRIAKAKIS, E., CHARMPILAS, N. & TAVERNARAKIS, N. 2017. Differential adiponectin
475 signalling couples ER stress with lipid metabolism to modulate ageing in C. elegans.
476 *Sci Rep,* 7**,** 5115.
477 LABBADIA, J. & MORIMOTO, R. I. 2014. Proteostasis and longevity: when does aging really
478 begin? *F1000Prime Rep,* 6**,** 7.

479 LEHNE, G. 2000. P-glycoprotein as a drug target in the treatment of multidrug resistant
480 cancer. *Curr Drug Targets,* 1**,** 85-99.
481 LIBERT, S., ZWIENER, J., CHU, X., VANVOORHIES, W., ROMAN, G. & PLETCHER, S. D. 2007.
482 Regulation of Drosophila life span by olfaction and food-derived odors. *Science,* 315**,**
483 1133-7.
484 LINCKE, C. R., BROEKS, A., THE, I., PLASTERK, R. H. & BORST, P. 1993. The expression of two
485 P-glycoprotein (pgp) genes in transgenic Caenorhabditis elegans is confined to
486 intestinal cells. *EMBO J,* 12**,** 1615-20.
487 LINDBLOM, T. H., PIERCE, G. J. & SLUDER, A. E. 2001. A C. elegans orphan nuclear receptor
488 contributes to xenobiotic resistance. *Curr Biol,* 11**,** 864-8.
489 LOPEZ-OTIN, C., BLASCO, M. A., PARTRIDGE, L., SERRANO, M. & KROEMER, G. 2013. The
490 hallmarks of aging. *Cell,* 153**,** 1194-217.
491 MAGNER, D. B., WOLLAM, J., SHEN, Y., HOPPE, C., LI, D., LATZA, C., ROTTIERS, V., HUTTER, H.
492 & ANTEBI, A. 2013. The NHR-8 nuclear receptor regulates cholesterol and bile acid
493 homeostasis in C. elegans. *Cell Metab,* 18**,** 212-24.
494 MATAI, L., SARKAR, G. C., CHAMOLI, M., MALIK, Y., KUMAR, S. S., RAUTELA, U., JANA, N. R.,
495 CHAKRABORTY, K. & MUKHOPADHYAY, A. 2019. Dietary restriction improves
496 proteostasis and increases life span through endoplasmic reticulum hormesis. *Proc*
497 *Natl Acad Sci U S A,* 116**,** 17383-17392.
498 MEISEL, J. D., PANDA, O., MAHANTI, P., SCHROEDER, F. C. & KIM, D. H. 2014.
499 Chemosensation of bacterial secondary metabolites modulates neuroendocrine
500 signaling and behavior of C. elegans. *Cell,* 159**,** 267-80.
501 MENEZ, C., ALBERICH, M., COURTOT, E., GUEGNARD, F., BLANCHARD, A., AGUILANIU, H. &
502 LESPINE, A. 2019. The transcription factor NHR-8: A new target to increase ivermectin
503 efficacy in nematodes. *PLoS Pathog,* 15**,** e1007598.
504 MENEZ, C., ALBERICH, M., KANSOH, D., BLANCHARD, A. & LESPINE, A. 2016. Acquired
505 Tolerance to Ivermectin and Moxidectin after Drug Selection Pressure in the
506 Nematode Caenorhabditis elegans. *Antimicrob Agents Chemother,* 60**,** 4809-19.
507 PAGE, A. P. 2018. The sensory amphidial structures of Caenorhabditis elegans are involved in
508 macrocyclic lactone uptake and anthelmintic resistance. *Int J Parasitol,* 48**,** 1035-
509 1042.
510 PARODI, A. J. 2000. Role of N-oligosaccharide endoplasmic reticulum processing reactions in
511 glycoprotein folding and degradation. *Biochem J,* 348 Pt 1**,** 1-13.
512 PERENS, E. A. & SHAHAM, S. 2005. C. elegans daf-6 encodes a patched-related protein
513 required for lumen formation. *Dev Cell,* 8**,** 893-906.
514 RICHARDSON, C. E., KOOISTRA, T. & KIM, D. H. 2010. An essential role for XBP-1 in host
515 protection against immune activation in C. elegans. *Nature,* 463**,** 1092-5.
516 RIERA, C. E., TSAOUSIDOU, E., HALLORAN, J., FOLLETT, P., HAHN, O., PEREIRA, M. M. A.,
517 RUUD, L. E., ALBER, J., THARP, K., ANDERSON, C. M., BRONNEKE, H., HAMPEL, B.,
518 FILHO, C. D. M., STAHL, A., BRUNING, J. C. & DILLIN, A. 2017. The Sense of Smell
519 Impacts Metabolic Health and Obesity. *Cell Metab,* 26**,** 198-211 e5.
520 SANGSTER, N. C. 1994. P-glycoproteins in nematodes. *Parasitol Today,* 10**,** 319-22.
521 SHEN, X., ELLIS, R. E., LEE, K., LIU, C. Y., YANG, K., SOLOMON, A., YOSHIDA, H., MORIMOTO,
522 R., KURNIT, D. M., MORI, K. & KAUFMAN, R. J. 2001. Complementary signaling
523 pathways regulate the unfolded protein response and are required for C. elegans
524 development. *Cell,* 107**,** 893-903.

525 SHEPS, J. A., RALPH, S., ZHAO, Z., BAILLIE, D. L. & LING, V. 2004. The ABC transporter gene
526 family of Caenorhabditis elegans has implications for the evolutionary dynamics of
527 multidrug resistance in eukaryotes. *Genome Biol,* 5**,** R15.
528 TAKATSUKI, A., ARIMA, K. & TAMURA, G. 1971. Tunicamycin, a new antibiotic. I. Isolation
529 and characterization of tunicamycin. *J Antibiot (Tokyo),* 24**,** 215-23.
530 TAYLOR, R. C. & DILLIN, A. 2013. XBP-1 is a cell-nonautonomous regulator of stress
531 resistance and longevity. *Cell,* 153**,** 1435-47.
532